Molecular and Histopathological Data on Levisunguis subaequalis Curran, Overstreet, Collins & Benz, 2014 (Pentastomida: Eupentastomida: Porocephalida: Porocephaloidea: Sebekidae: Sebekinae) from Gambusia affinis in Alabama, USA

Authors: Woodyard, Ethan T., Stilwell, Justin M., Camus, Alvin C., and Rosser, Thomas G.

Source: Journal of Parasitology, 105(6) : 827-839

Published By: American Society of Parasitologists

URL: https://doi.org/10.1645/19-38

Journal of Parasitology 2019 105(6) 827–839

Published 19 November 2019

DOI: 10.1645/19-38

Contents and archives available through www.bioone.org or www.jstor.org

Journal of Parasitology

journal homepage: www.journalofparasitology.org

MOLECULAR AND HISTOPATHOLOGICAL DATA ON *LEVISUNGUIS SUBAEQUALIS* CURRAN, OVERSTREET, COLLINS & BENZ, 2014 (PENTASTOMIDA: EUPENTASTOMIDA: POROCEPHALIDA: POROCEPHALOIDEA: SEBEKIDAE: SEBEKINAE) FROM *GAMBUSIA AFFINIS* IN ALABAMA, USA

Ethan T. Woodyard[1], Justin M. Stilwell[2], Alvin C. Camus[2], and Thomas G. Rosser[1]

[1] Department of Basic Sciences, College of Veterinary Medicine, Mississippi State University, Mississippi State, Mississippi 39762.
[2] Department of Pathology, College of Veterinary Medicine, University of Georgia, Athens, Georgia 30602.
Correspondence should be sent to Ethan T. Woodyard at: *etw35@msstate.edu*

KEY WORDS

Gambusia affinis
Levisunguis subaequalis
Pentastome
Western Mosquitofish
Systematics

ABSTRACT

Levisunguis subaequalis Curran, Overstreet, Collins & Benz, 2014, was recently described from the lungs of the definitive hosts, softshell turtles, *Apalone ferox* (Schneider, 1783), and *Apalone spinifera aspera* (Agassiz, 1857) as well as the viscera of an intermediate host, the western mosquitofish, *Gambusia affinis* (Baird and Girard, 1853). However, the original account lacked molecular data. Furthermore, histological examination of infected host tissues in the original account of *L. subaequalis* did not reveal any pathological changes in the intermediate host. The present work provides a robust morphological description of the nymph and novel molecular data from the *18S* and *28S* ribosomal gene regions and the cytochrome *c* oxidase subunit 1 (*COI*) mitochondrial gene. Phylogenetic analyses using Bayesian inference and maximum likelihood analysis with concatenated sequence data from these 3 regions, as well as each region individually, placed the turtle pentastomid *L. subaequalis* as a sister clade to the crocodilian pentastomids of the genus *Sebekia* Sambon, 1922. While only concatenated phylogenetic analyses agreed with the currently accepted classification of the Eupentastomida and phylogenetic signal assessment indicated that the concatenated data set yielded the most phylogenetic signal, data from more taxa are still needed for robust phylogenetic inferences to be made. The intensity of infection ranged from 2 to 171 nymphs per fish, compared with the highest previously reported intensity of 6. These high-intensity infections with *L. subaequalis* were characterized by the nymphs occupying 5–50% of the coelomic cavity of *G. affinis*. However, despite this heavy parasite infection, fish exhibited minimal pathology. Observed pathology was characterized by compression or effacement of organs adjacent to the nymphs, particularly liver, swim bladder, and intestines, as well as the formation of granulomas around shed pentastomid cuticles. Nonetheless, the morphological and molecular data provided in the present work will bolster future efforts to identify this pentastomid in other hosts where pathology may be present in addition to aiding in the advancement of the field of molecular pentastomid systematics.

Eupentastomida Waloszek, Repetski & Maas, 2006, is an enigmatic class of the extant crustacean endoparasites of the phylum Pentastomida Huxley, 1869, with adults infecting the respiratory tracts or lungs of mammalian, reptilian, or avian definitive hosts and nymphs generally encysted in vertebrate or invertebrate intermediate hosts (Christoffersen and de Assis, 2015). The nomenclature of pentastomids is characterized by a number of taxonomic anomalies including misspelled taxa, incorrect attributions of taxonomic authority names and dates, and incorrectly nominated type species, as recently cataloged and corrected by Poore (2012). The systematics of this class have culminated in the present classification system of Christoffersen and de Assis (2013), which recognizes 141 nominal species in 26 genera. This system was derived by combining previous morphology-based phylogenies of pentastomids by Almeida and Christoffersen (1999) and Junker (2002). While the aforementioned authors have invested considerable effort into resolving the nomenclature of pentastomids and relationships between pentastomid taxa using morphological characters, application of molecular techniques may further clarify these relationships. Both the adult and the nymph of the pentastomid *Levisunguis subaequalis* Curran, Overstreet, Collins & Benz, 2014, have been recently described (Curran et al., 2014). Adults were described from the Gulf Coast spiny softshell turtle, *Apalone spinifera*

Figure 1. Ventral surface of a *Gambusia affinis* (Baird and Girard, 1853) heavily infected with nymphal *Levisunguis subaequalis* Curran, Overstreet, Collins & Benz, 2014.

aspera (Agassiz, 1857), and the Florida softshell turtle, *Apalone ferox* (Schneider, 1783), while the nymph was described from the western mosquitofish, *Gambusia affinis* (Baird and Girard, 1853). Additionally, nymphs of *Levisunguis* sp., identified only at the genus level, have been reported from *G. affinis* by Carpenter (2018). Although morphological data are available for the adult of both sexes and to a lesser extent the nymph of *L. subaequalis,* there are at present no molecular data for this species. Also, no description of pathological effects associated with infection in the intermediate host is presently available. Furthermore, while this species was described immediately after the publication of the currently accepted classification of pentastomids, the phylogenetic placement of *Levisunguis* in this system is not clear because Christoffersen and de Assis could not reference the as-yet-undescribed *L. subaequalis*. The present work provides the first molecular data for this species and tentative phylogenetic analyses used to infer the placement of *L. subaequalis* within the context of current pentastomid systematics. Phylogenetic signal assessment was also carried out to assess the relative taxonomic utility of *18S* and *28S* ribosomal genes and the cytochrome *c* oxidase subunit 1 (*COI*) mitochondrial gene as well as concatenated alignments of all 3 loci. Also provided is a detailed morphological description of the nymph and a description of pathologic changes associated with high-intensity infections in the only identified intermediate host, *G. affinis*. These data will bolster future identification of this pentastomid and aid in inferring the evolutionary history of pentastomids by allowing for more robust phylogenetic analyses.

MATERIALS AND METHODS

Parasite collection

In July 2018, 44 specimens of *G. affinis* were collected via hand netting from an ornamental pond in Birmingham, Alabama. Fish were morphologically identified as *G. affinis* and not *Gambusia holbrooki* Girard, 1859, according to Boschung and Mayden (2004) based on the presence of 6 dorsal fin rays, 9 anal fin rays, 12 pectoral fin rays, and 13 caudal fin rays (Suppl. Fig. S1). Several of these fish were visibly infected with endoparasites (Fig. 1). These fish were transported to the Aquatic Parasitology Lab at Mississippi State University's College of Veterinary Medicine for parasitological examination as part of a routine diagnostic investigation. Fish were euthanized with an overdose of MS-222 (Western Chemical Inc., Ferndale, Washington). Eight fish were individually dissected in 0.9% physiological saline in glass dishes under a dissecting microscope to collect parasites. Afterward, the dissected fish remnants were individually digested by incubation at 40 C for 3 hr in 500-ml Erlenmeyer flasks with 200 ml of 0.5% pepsin solution acidified with citric acid (Kim et al., 2013). The contents of each flask were then screened in brass sieves with a 25-μm aperture. Screened contents were examined in glass dishes under a dissecting microscope to collect any parasites not collected during the initial necropsy. All collected parasites, from both necropsies and pepsin digestion, were identified as nymphal pentastomids and fixed directly in 70% ethanol for morphological and molecular characterization. The abdominal cavities of 20 additional *G. affinis* were injected with 10% neutral-buffered formalin (NBF), and the whole fish were fixed directly in 10% NBF for histopathology.

Abundance, intensity, and prevalence

Abundance, intensity, and prevalence, as defined by Bush et al. (1997), were calculated for *L. subaequalis* collected from *G. affinis* using Quantitative Parasitology 3.0 (Rózsa et al., 2000) with 95% confidence limits calculated using the Clopper-Pearson Method (Clopper and Pearson, 1934) with 2,000 bootstrap replications.

Morphological characterization

Three hologenophores of nymphal *L. subaequalis* were made using the methods described by Woodyard et al. (2019a). Briefly, the cephalothorax was cut from each individual nymph using a sterile scalpel blade. The removed cephalothorax was then dehydrated in a series of 4 ethanol washes (70–100%), cleared in methyl salicylate, and mounted on a glass slide in Canada balsam. Each corresponding hindbody was then placed in 1.5-ml tubes with 180 μl of Buffer ATL (Qiagen, Hilden, Germany) and 20 μl of proteinase K and incubated overnight at 55 C. The hindbody was recovered, dehydrated in a series of 4 ethanol washes from 70–100%, cleared in methyl salicylate, and mounted on the same slide as the corresponding cephalothorax. Ten nymphal paragenophores were also made using the above methods without DNA extraction. Three additional nymphs were directly mounted in Hoyer's medium (Hempstead Halide, Galveston, Texas) to better visualize chloride pores, which were not as easily seen in nymphs mounted in Canada balsam. Additionally, the oral cadre was excised from each of the 2 nymphs with scalpel blades and mounted directly in Hoyer's medium to compare with the excised oral cadre according to Curran et al. (2014). Hook and oral cadre measurement schemes were adapted from Fain (1961) (Fig. 2).

Histopathological evaluation

Twenty formalin-fixed fish were decalcified in Kristensen's solution for 3 hr, serially trimmed in transverse sections or longitudinally bisected dorsoventrally along the midline, placed into individual tissue cassettes, and processed routinely. Paraffin-embedded tissues were sectioned at 4 μm, adhered to positively charged slides, and stained with hematoxylin and eosin. An additional section of 1 fish was stained with Verhoeff van Gieson stain, an alternative to Movat's pentachrome for highlighting the sclerotized openings of pentastomids, according to previously published methods (Sheehan and Hrapchak, 1980).

Molecular characterization and phylogenetic analysis

DNA was extracted from 3 hologenohpores and 1 whole nymph (DNeasy Blood and Tissue Kit, Qiagen, Hilden, Germany). The *18S* and *28S* ribosomal RNA gene regions were

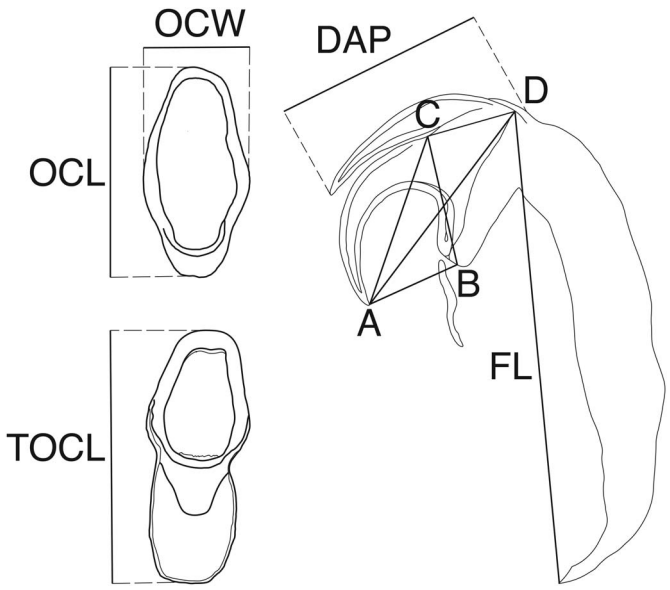

Figure 2. Line drawings of taxonomically informative structures of nymphs of *Levisunguis subaequalis* Curran, Overstreet, Collins & Benz, 2014, mounted in Hoyer's medium. In situ oral cadre and measurement scheme for length and width. Oral cadre measurements are as follows: TOCL, total excised oral cadre length, OCL, oral cadre length and OCW, oral cadre width. Hook and fulcrum measurement schemes as follows: AC, blade length; AD, hook length; BC, base length; AB, hook gape; CD, plateau length; FL, fulcrum length; DAP, nymphal accessory piece length, ventral view.

amplified and sequenced using previously published primers (Table I) and thermal cycling parameters (Table II). New primers were designed to facilitate the amplification of a partial *COI* gene sequence from pentastomids in the present study. Additionally, partial *COI* from *G. affinis* was amplified using the LCO1490/HCO2198 primer set. The fin from an infected *G. affinis* (Fig. 1) was removed, and DNA was extracted as above. A section of the trunk of an additional *G. affinis* (Suppl. Fig. S1) was also subjected to DNA extraction. PCR was carried out using extracted DNA from *G. affinis* to molecularly confirm host species identity and aid in the design of pentastomid-specific *COI* primers. PCR reactions consisted of 10 µl of Phusion Hot Start II High-Fidelity PCR Master Mix (Thermofisher Scientific, Waltham, Massachusetts), 1 µl of each primer (10 nmol), 7 µl of nuclease-free water, and 1 µl of DNA template (~10 ng). PCR products were visualized by electrophoretic migration in 0.8% agarose gels buffered with sodium borate and stained with ethidium bromide. Amplicons were excised, purified (Qiagen Gel Extraction Kit, Qiagen), and bidirectionally sequenced using the same primers used for amplification (Eurofins Genomics, Louisville, Kentucky). The resultant electropherograms were assembled into contiguous sequences in Geneious 11.1.5 (Kearse et al., 2012) and checked for ambiguities. Pentastomid sequences for the *18S, 28S,* and *COI* regions generated in the present study were aligned with all available sequences of pentastomids downloaded from GenBank. Sequences that contained ambiguous bases and those that would not allow the alignments to be trimmed owing to insufficient overlap with other sequence data were excluded from the analyses. Sequences used in the present analyses are indicated in Suppl. Table S1. Separate alignments were generated for each of these loci using GUIDANCE2's implementation of the MAFFT algorithm (Katoh and Standley, 2013) on the GUIDANCE2 Web Server (Landan and Graur, 2008; Sela et al., 2015). Isolates for which data from all 3 loci were available were also used for concatenated phylogenetic analyses. Once constructed, alignments were trimmed manually, and all sites containing gaps were removed in Geneious. Single-locus alignment lengths were as follows: *18S* (238 bp), *28S* (941 bp), *COI* (157 bp). Alignment lengths for each region in the concatenated analyses were as follows: *18S* (1,191 bp), *28S* (1,014 bp), and *COI* (650 bp), for a total alignment of 2,855 base pairs. The disparity in alignment lengths for single loci between the concatenated and single-locus phylogenies is due to the inconsistency of sequence quality and length of sequences available in GenBank for pentastomids. Optimum DNA substitution models were determined for the *18S* and *28S* alignments as well as each codon position in the *COI* alignments using the Bayesian Information Criterion in MEGA7 (Kumar et al., 2016). Additionally, substitution saturation indices were calculated for each codon position in both *COI* alignments using DAMBE v. 7.0.13 (Xia, 2018) to ensure that the phylogenetic utility of these data was not adversely affected by substitution saturation. Substitution models for each locus in the single-locus alignments were as follows: *18S* (K2+G), *28S* (T92+G), *COI* codon position 1 (TN93), *COI* codon position 2 (T92+G), and *COI* codon position 3 (JC). Substitution models for each locus for the concatenated alignment were as follows: *18S* (K2+G), *28S* (K2+G), *COI* codon position 1 (HKY+G), *COI* codon position 2 (HKY), and *COI* codon position 3 (T92+I). These alignments were then concatenated in MEGA7, and a

Table I. Primers used for DNA amplification.

Primer name	Primer sequence (5′–3′)	Gene target	Reference
18S_1F	ACCTGGTTGATCCTGCCAGT	*18S*	Barton and Morgan, 2016
18S_1000F	CGATCAGATACCGCCCTAGTTC	*18S*	Dreyer and Wägele, 2001
18S_1800R	GATCCTTCCGCAGGTTCACCTACG	*18S*	Raupach et al., 2009
LSU5	TAGGTCGACCCGCTGAAYTTAAGCA	*28S*	Littlewood et al., 2000
1500R	GCTATCCTGAGGGAAACTTCG	*28S*	Tkach et al., 2003
28S 4759F	GTCTTGAAACACGGACCAAG	*28S*	Rosser et al., 2017
28S 5699R	TACCACCAAGATCTGCACCT	*28S*	Rosser et al., 2017
LCO1490	GGTCAACAAATCATAAAGATATTGG	*CO1*	Folmer et al., 1994
HCO2198	TAAACTTCAGGGTGACCAAAAAAT	*CO1*	Folmer et al., 1994
Cox1_Internal_F	TTAGCCGCTCATCCCCTAGTAT	*CO1*	Present study
Cox1_Internal_R1	GAGATTTGGGATAGGGATGATTTA	*CO1*	Present study

Table II. Thermal cycling parameters used for DNA amplification.

Primer	Denaturation	Cycling	Extension/elongation
18S_1F/18S_1800R 18S_1000F/18S_1800R	98 C; 3 min	35 cycles of 98 C for 10 sec, 53 C for 30 sec, 72 C for 1 min	72 C; 10 min
LSU5/1500R	98 C; 3 min	45 cycles of 98 C for 10 sec, 57 C for 30 sec, 72 C for 1 min	72 C; 10 min
28S 4759R/28S 5699R	98 C; 3 min	35 cycles of 98 C for 10 sec, 58 C for 30 sec, 72 C for 1 min	72 C; 10 min
LCO1490/HCO2198 LCO1490/Cox1_Internal_R1 Cox1_Internal_F/HCO2198	98 C; 3 min	35 cycles of 98 C for 10 sec, 48 C for 30 sec, 72 C for 1 min	72 C; 10 min

partitioned, concatenated Bayesian phylogenetic analysis was performed in MrBayes 3.2.6 (Ronquest and Huelsenbeck, 2003; Altekar et al., 2004) using Markov chain Monte Carlo searches of 2 simultaneous runs of 4 chains with sampling of 100th tree for 1×10^6 generations, ensuring the value of the standard deviation of the split frequencies reached <0.1. In addition to Bayesian phylogenetic inference, maximum likelihood analysis was conducted on the same alignments with the aforementioned partitioning scheme and models using IQ-Tree (Nguyen et al., 2015) on the IQ-Tree Web Server (Trifinopoulos et al., 2016). Single-locus analyses were carried about using the above methods with the exception of not being concatenated in MEGA7 prior to analyses by MrBayes and IQ-Tree. In addition to the aforementioned molecular methods of tree construction, a cladogram of the currently accepted morphology-based classification of pentastomids, with the addition of the genus *Levisunguis,* was constructed using a text editor. Trees constructed in MrBayes and IQ-Tree, as well as the cladogram constructed via a text editor, were formatted in FigTree 1.4.3 (Rambaut, 2016) and Adobe Illustrator 23.0.2.

To assess the similarity of molecular data from *L. subaequalis* and other molecularly characterized pentastomid species, *18S, 28S,* and *COI* sequences for *L. subaequalis* in the present study were searched in the GenBank, and up to the 10 closest nominal species matches, where data availability allowed, were downloaded and aligned as above. Geneious was then used to assess distances between these sequences.

To assess the relative phylogenetic utility of each of the aforementioned gene targets, phylogenetic informativeness profiles were constructed using PhyDesign (López-Giráldez and Townsend, 2011). The phylogenetic tree constructed using the concatenated alignment was formatted with FigTree, arbitrarily ultrametricized with Mesquite (Maddison and Maddison, 2018), and uploaded to the PhyDesign web server along with the concatenated, partitioned alignment file used in the concatenated phylogenetic analyses. The resultant phylogenetic informativeness profile images were formatted with Adobe Illustrator 23.0.2.

RESULTS

Intensity, abundance, and prevalence

Levisunguis subaequalis was detected in 100% (8/8) of dissected *G. affinis*. Intensity ranged from 2 to 171 nymphs with a mean intensity of 36.8 (95% bootstrap confidence limit 12.8–112).

Morphological characterization

Measurements from 18 nymphs: Reported measurements are rounded to the nearest micron unless otherwise stated and in the following format: range (average) Body 6.00–7.88 (6.77) mm long with 65–76 (71) annuli (Fig. 3). Oral cadre open anteriorly, 125–223 × 92–111, in situ (Fig. 4A). Excised oral cadre total length 300–320 (322) (n = 2) (Fig. 4B). Each hook bearing a sclerotized accessory piece (Fig. 4C). Fine, cuticular spines continuous along posterior of each annulus. Chloride pores 6–8 (7) in diameter, arranged in 2–3 irregular, horizontal rows along the middle each annulus (Fig. 4D). Hook and fulcrum measurements, compared with those of nymphs of *Sebekia mississippiensis* Overstreet, Self & Vliet, 1985, are indicated in Table III. Measurements from individual nymphs provided in Suppl. Table S2. Vouchers are deposited in the Harold W. Manter Laboratory of Parasitology, University of Nebraska, Lincoln, Nebraska under the following accession numbers:

Table III. Comparative morphological data for nymphs of *Levisunguis subaequalis* from the present study and *Sebekia mississippiensis* (Woodyard et al., 2019a).*

Hook position	AC	AD	BC	CD	AB	FL	DAP
Levisunguis subaequalis (Present study, n = 16)							
RA	131–171 (153)	137–189 (162)	83–121 (108)	69–91 (82)	72–90 (78)	302–405 (354)	146–186 (171)
LA	114–172 (153)	142–176 (158)	94–129 (110)	70–94 (81)	69–95 (79)	318–371 (355)	146–200 (176)
RP	125–179 (150)	139–169 (152)	89–118 (106)	67–92 (80)	66–84 (74)	323–362 (343)	144–205 (175)
LP	125–164 (148)	137–174 (154)	91–120 (106)	66–95 (83)	65–84 (73)	301–368 (345)	151–200 (180)
Sebekia mississippiensis (Woodyard et al., 2019a, n = 11)							
All	65–91 (81)	76–94 (87)	42–53 (49)	—	27–45 (39)	126–216 (169)	74–99 (84)

* Measurements reported in micrometers in the following format: range (average). Hook positions: RA: right anterior, LA: left anterior, RP: right posterior, LP: left posterior, All: average of hook measurements. Features: AC: blade length, AD: hook length, BC: base length, AB: hook gape, FL: fulcrum length, DAP: dorsal accessory piece length.

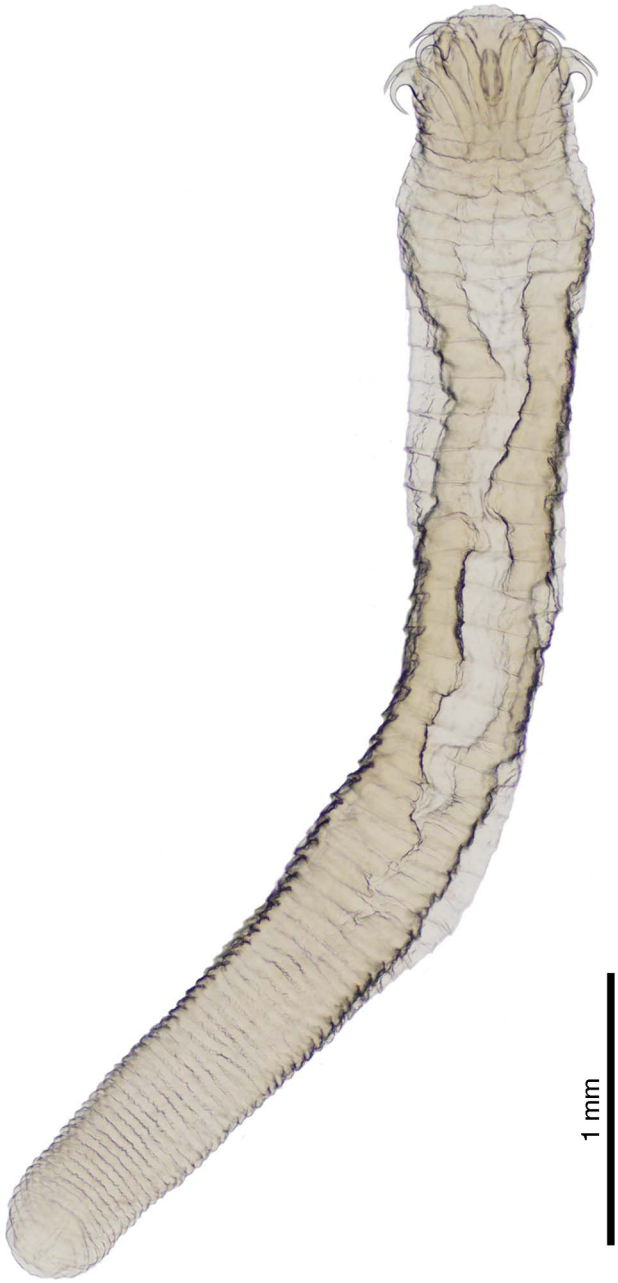

Figure 3. Nymph of *Levisunguis subaequalis* Curran, Overstreet, Collins & Benz, 2014, from *Gambusia affinis* (Baird and Girard, 1853) mounted in Hoyer's medium. Color version available online.

hologenophores (HWML210023–HWML210025) and parageno-phores (HWML210027–HWML210036).

Histopathological description of *Levisunguis subaequalis* in *Gambusia affinis*

Nymphs of *L. subaequalis* were detected in 55% (11/20) of fish examined by light microscopy. All infected fish were gravid females. The nymphs occupied approximately 5–50% of the coelomic cavity by visual estimation, either free or encapsulated in pseudocysts formed by a few layers of epithelioid macrophages and fibroblasts (Fig. 5). The pentastomids typically compressed, dissected between, or displaced adjacent organs, particularly liver lobules, the swim bladder, and intestinal loops in all infected fish (Fig. 5). Aside from hepatocellular atrophy, coelomic distension, and moderate to severe thinning and atrophy of the ventral body wall musculature, no significant pathology was seen in the host viscera. The cephalothorax region of the pentastomids contained 2 pairs of retracted, curved, refractile hooks surrounded by skeletal myofibers (Fig. 6A). Bilaterally symmetric, tortuous head glands and hemolymph flanked the cephalic ganglion and esophagus (Fig. 6B). The glands produced a homogeneous, eosinophilic material (presumptive chitinous cuticle). The esoph-ageal lumen of each specimen contained deep brown pigment consistent with hematin from digested host erythrocytes (Fig. 6B). Large acidophilic glands persisted down the length of the nymph along with thin peripheral bands of skeletal muscle, abundant vacuolated space, multifocal basophilic cells, and an intestine (Fig. 6C, D). The body of each nymph was pseudosegmented and lined by a chitinous cuticle with randomly distributed sclerotized openings containing annular rings, which stained black with Verhoeff van Gieson stain (Fig. 6C–F). The cuticle was occasionally shed, which incited infiltrates of epithelioid macro-phages and granuloma formation in the mesentery. In fewer numbers within the mesentery of some fish, smaller granulomas contained acanthocephalans and larval nematodes, whereas the intestinal lumen occasionally contained adult nematodes. A slide used for histological assessment in the present study is deposited in Harold W. Manter Laboratory of Parasitology, University of Nebraska, Lincoln, Nebraska (HMWL-210026).

Molecular characterization and phylogenetic analysis

While Bayesian inference and maximum likelihood phyloge-netic analyses of ribosomal *18S* and *28S* regions and the mitochondrial *COI* gene all suggested a close evolutionary relationship between *Levisunguis,* as a distinct clade, and species of *Sebekia,* these trees exhibited low posterior probabilities and bootstrap support values as well as polytomies, polyphyletic clades, and general disagreement of topology with the current classification of pentastomids (Suppl. Figs. 2–4). Concatenated analyses using all 3 regions also resulted in trees with low support values and placed sequences of *Levisunguis* as a sister clade to the sebekid pentastomids, which use crocodilian definitive hosts. Together, these 2 groups form a clade for the subfamily Sebekinae. The placement of genera in these concatenated phylogenetic analyses is in accord with the currently accepted, morphology-based organization of the Eupentastomida (Fig. 7), while the single-locus analyses did not agree with each other or the morphology-based classification. *Levisunguis subaequalis* sequences from the present study are deposited in GenBank under the following accession numbers: *18S* (MN065566–MN065569), *28S* (MN065506–MN065509), and *COI* (MN062093–MN062096). The *G. affinis COI* sequences from the present study are deposited under the following GenBank accession numbers: MN265387–MN265388.

Percentage similarity between *18S, 28S,* and *COI* sequences for *L. subaequalis* from the present study and up to the 10 closest nominal species matches from GenBank are presented in Table IV. Sequences for *L. subaequalis* were 100% similar to each other for each gene. *18S* showed the least variability between species, followed by *28S* and *COI*. Given that no fewer than 4 species were

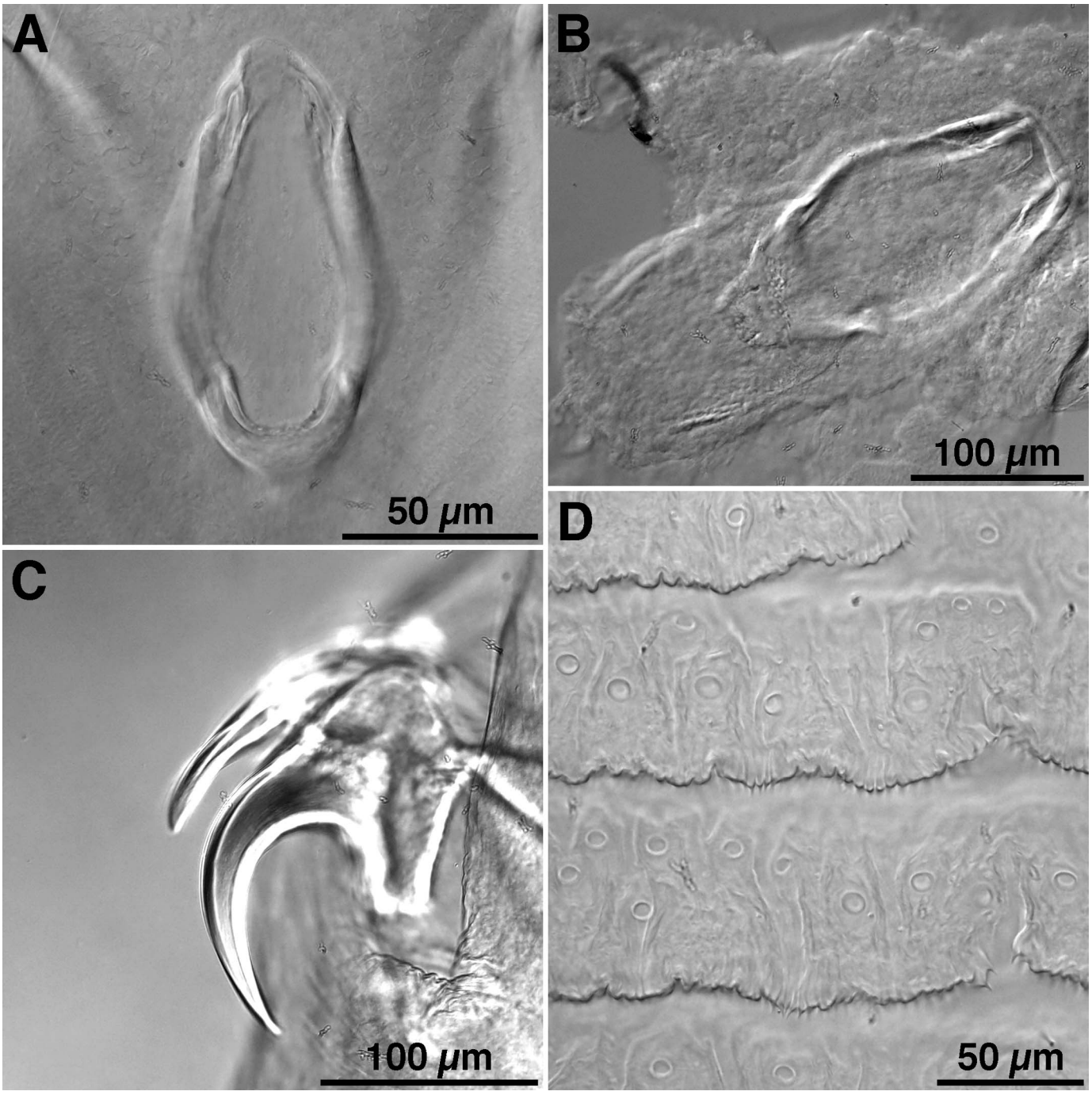

Figure 4. Photomicrographs of qualitative characters of ventrally mounted nymphs of *Levisunguis subaequalis* Curran, Overstreet, Collins & Benz, 2014 mounted in Hoyer's medium. (**A**) In situ oral cadre. (**B**) Excised oral cadre. (**C**) Hook and dorsal accessory piece. (**D**) Annuli showing fine cuticular spines continuous along posterior of each annulus on posterior margin and chloride pores arranged in irregular rows of 2–3 on each annulus.

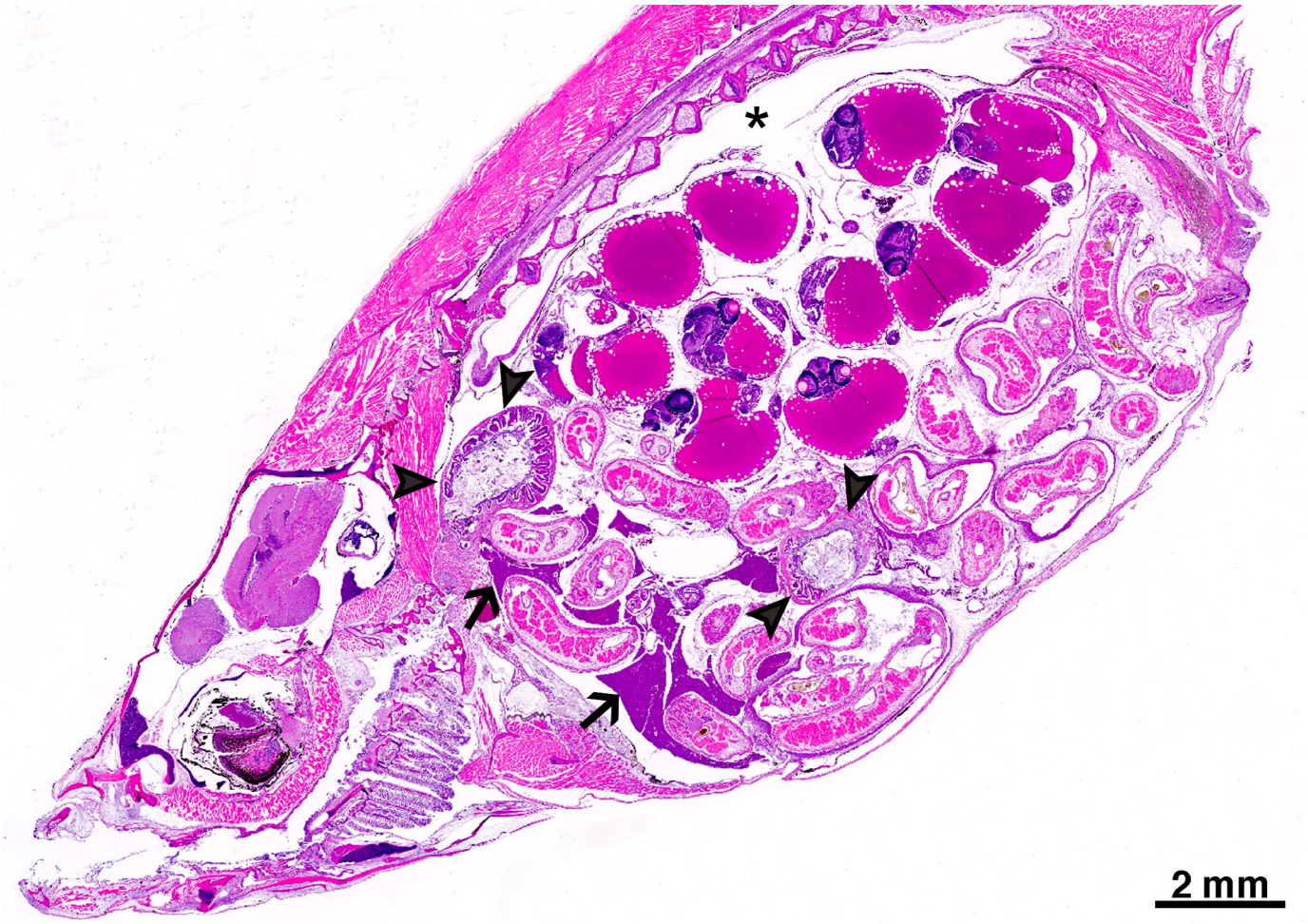

Figure 5. Subgross magnification of a longitudinal, midline section through the body of a *Gambusia affinis* (Baird and Girard, 1853). Nymphs of *Levisunguis subaequalis* Curran, Overstreet, Collins & Benz, 2014, fill approximately 50% of the coelom and compress the liver (arrows), intestine (arrowheads), and swim bladder (asterisk). H&E stain. Color version available online.

≥99% similar at *18S,* this gene is likely not suited for identification of pentastomids to species.

Phylogenetic signal analysis carried out on the concatenated *18S, 28S,* and *COI* alignment suggests that the concatenated dataset yields more net phylogenetic signal than *18S, 28S,* or *COI* alone. Regarding the individual loci, *28S* offers greater signal at the basal end of the tree while *COI* offers slightly greater support at more distal clades. *18S* offered comparatively little phylogenetic signal throughout (Fig. 8).

DISCUSSION

Nymphs in the present study were found to be morphologically consistent with the description of *L. subaequalis* by Curran et al. (2014), though these authors' description of taxonomically informative hook measurements as "similar in morphology to adult hooks but smaller" complicates efforts to make comparisons. Given that no nymphal vouchers have been deposited for this species, direct comparison with nymphs from the present study is not possible. Nonetheless, the nymphs from the present study agree in annulus counts, chloride pore diameter and distribution, fulcrum lengths, and oral cadre dimensions. Furthermore, the ranges of taxonomically informative hook measurements for *L. subaequalis* and *Sebekia mississippiensis,* the only other nominal sebekid reported from *G. affinis* in the southeastern United States (Curran et al. 2014), do not overlap to any degree (Table III). Given that nymphs from the present study are morphologically consistent with *L. subaequalis* and not with *S. mississippiensis,* the pentastomids in the present study are identified as *L. subaequalis*. Although Curran et al. (2014) placed *L. subaequalis* in the family Sebekidae, the species was not placed within a subfamily. However, based on the distribution of chloride pores and the absence of an esophageal peg of the oral cadre, *L. subaequalis* is a member of the subfamily Sebekinae within the family Sebekidae. This is in accordance with the keys to genera provided by Christoffersen and de Assis (2013).

Also of note, the measurements for nymphs of *L. subaequalis* from the present study were more consistent with 1 of the nymphal specimens in the type series of *Sebekia mississippiensis* Overstreet, Self & Vliet 1985 (AMNH 538) than all other described nymphs of *S. mississippiensis*. Hook and fulcra measurements for this nymph were previously reported as follows: AB (42), AC (164), AD (171), BC (124), DAP (122), and fulcrum length (410) (see suppl. data table S1 in Woodyard et al., 2019a).

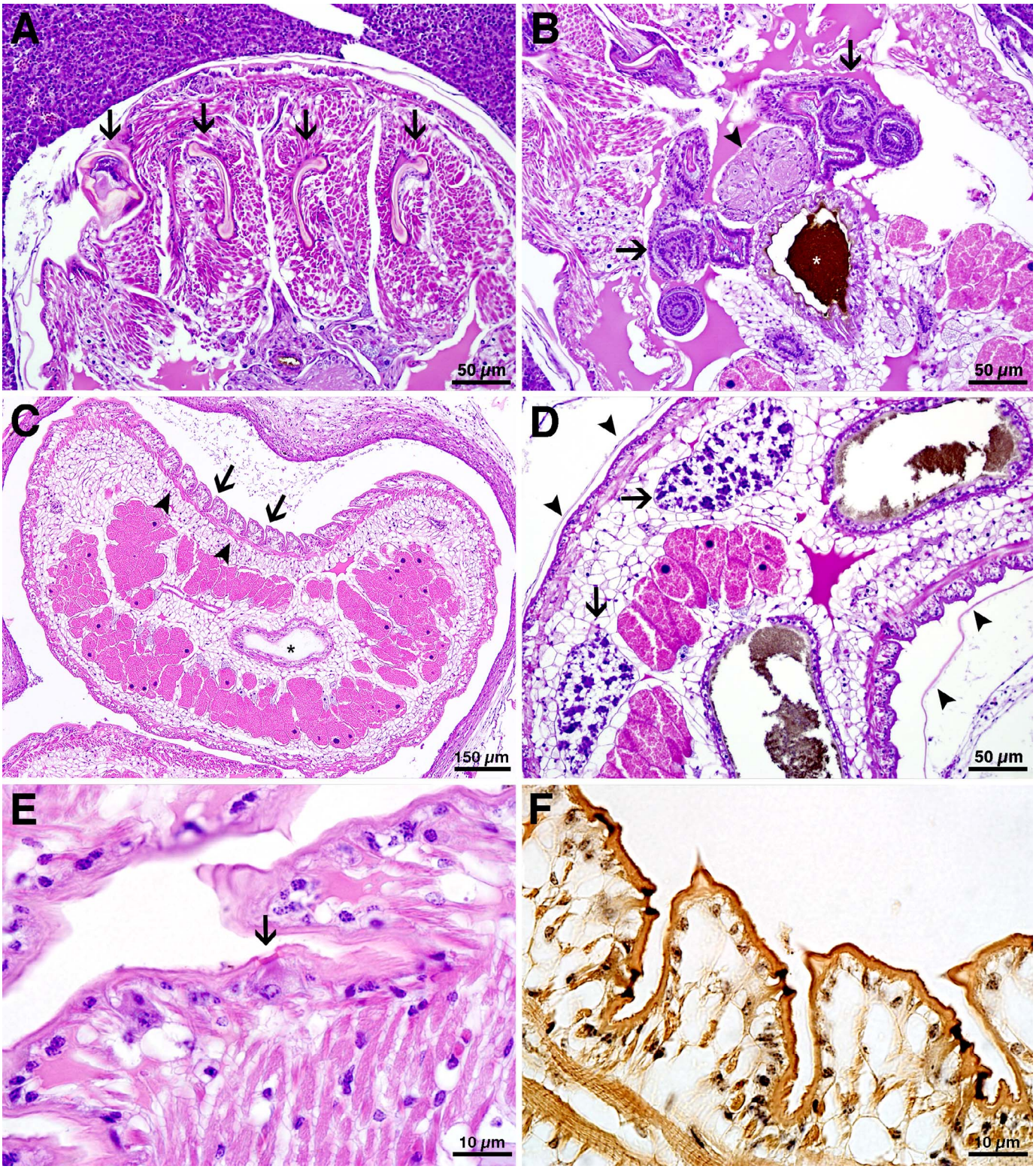

Figure 6. Structural features of nymphs of *Levisunguis subaequalis* Curran, Overstreet, Collins & Benz, 2014, infecting the coelom of *Gambusia affinis* (Baird and Girard, 1853) in longitudinal, transverse, and oblique sections. (**A**) Two pairs of refractile hooks (arrows) are retracted within the head of the nymph. H&E stain. (**B**) Within the head, a ganglion (arrowhead) and esophagus containing digested blood (white asterisk) are enclosed on either side by symmetrical head glands (arrows). H&E stain. (**C**) The body is pseudosegmented (arrows) with a thin layer of subcuticular skeletal muscle (arrowheads), central intestine (asterisk), and large acidophilic glands. H&E stain. (**D**) Multifocal clusters of basophilic cells are scattered throughout the body (arrows). Note the recently shed cuticle (arrowheads). H&E stain. (**E**) The cuticle contains randomly disseminated sclerotized openings with hyaline annular rings (arrow). H&E stain. (**F**) The annular rings stain black with an elastin stain (Verhoeff van Gieson stain). Color version available online.

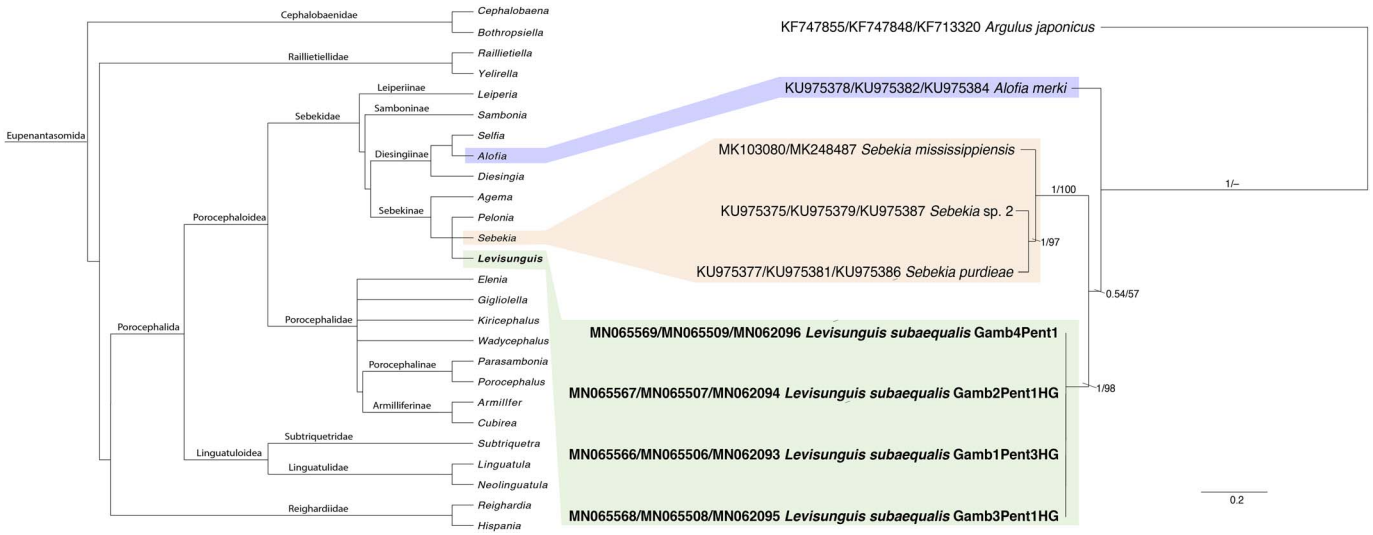

Figure 7. Cladogram depicting the currently accepted taxonomy of class Eupentastomida adapted from Christoffersen and de Assis (2013) to include *Levisunguis* based on keys provided therein and the description of *L. subaequalis* Curran, Overstreet, Collins & Benz, 2014, by Curran et al. (2014). The cladogram is juxtaposed with concatenated phylogenetic analyses from *18S, 28S,* and cytochrome *c* oxidase subunit 1 (*COI*) from *L. subaequalis* in the present study and available pentastomid sequences from GenBank. GenBank accession numbers are given for each sequence in the format *18S* accession number/*28S* accession number/*COI* accession number. Numbers above branches indicate Bayesian posterior probabilities/maximum likelihood bootstrap values. Scale bar represents the number of nucleotide substitutions per site. Color version available online.

Table IV. Percentage similarity between *18S, 28S,* and *COI* sequences for *Levisunguis subaequalis* from the present study compared with closest nominal species matches in GenBank. Percentages are based on 402, 378, and 215 base pair alignments for *18S, 28S,* and *COI,* respectively. Few *28S* sequences were available for comparison.

GenBank data	Present study
L. subaequalis 18S (MN065566–MN065569)	
Kiricephalus pattoni (KC904947)	99.51
Alofia merki (KU975378)	99.50
Sebekia mississippiensis (MK103080)	99.50
Sebekia purdieae (KU975377)	99.50
Porocephalus crotali (MG559607)	99.00
Waddycephalus radiata (MH194559)	98.51
Kiricephalus coarctatus (MG559634)	98.26
Armillifer moniliformis (HM048870)	98.26
Armillifer agkistrodontis (FJ607339)	98.01
Armillifer armillatus (KJ877184)	98.01
L. subaequalis 28S (MN065506–MN065509)	
Alofia merki (KU975382)	91.27
Sebekia mississippiensis (MK103080)	86.24
Sebekia purdieae (KU975381)	85.98
Armillifer armillatus (GQ886350)	51.06
L. subaequalis COI (MN062093–MN062096)	
Porocephalus crotali (MG559655)	78.60
Armillifer armillatus (AY456186)	76.74
Armillifer grandis (NC_037187)	75.35
Raillietiella hebitihamata (JF975594)	75.35
Raillietiella orientalis (MG559637)	74.88
Kiricephalus coarctatus (MG559658)	74.88
Armillifer agkistrodontis (KX686568)	74.88
Alofia merki (KU975384)	74.88
Sebekia purdieae (KU975386)	73.95
Sebekia mississippiensis (MK248489)	72.56

These data suggest that this specimen may be *L. subaequalis* rather than *S. mississippiensis*. Boyko (1996) indicates that this specimen, deposited in association with the original description of *S. mississippiensis* by Overstreet et al. (1985), is from *G. affinis* collected 4 miles east of Grand Chenier, Louisiana. This specimen likely represents a previously unacknowledged host record for *L. subaequalis*.

Given that the highest previously reported intensity for *L. subaequalis* in *G. affinis* is 6 (Curran et al., 2014), intensities in the present study of up to 171 nymphs per *G. affinis* were expected to induce significant pathologic changes in the host. However, limited adverse changes were observed in the present study, suggesting an old host-parasite relationship. Anecdotally, host motility appeared to have been negatively impacted given that fish were easily netted at the surface. The compression of the swim bladder by nymphs of *L. subaequalis,* as observed histologically in the present study, may have played some role here. However, such claims remain speculative in the absence of behavior studies comparing infected and uninfected *G. affinis*. Although the type intermediate host does not appear to be greatly affected by infection with *L. subaequalis,* potential infectivity and pathology of this pentastomid to other fish species remains unknown.

Different gene targets have varying efficacy for resolving taxonomic uncertainty at multiple taxonomic rankings (Hwang and Kim, 1999). Given the tumultuous history of pentastomid systematics, the recent, morphology-based reorganizations of the evolutionary relationships of pentastomids (Almeida and Christoffersen, 1999; Junker, 2002; Christoffersen and de Assiss, 2013) warrant confirmation using molecular data. However, the current dearth of sequence data suitable for such analyses confounds efforts at phylogenetic inference. Both single-locus Bayesian inference and maximum likelihood analyses using the *18S* (Suppl. Fig. S2), *28S* (Suppl. Fig. S3), and *COI* (Suppl. Fig. S4) regions as well as concatenated Bayesian and maximum

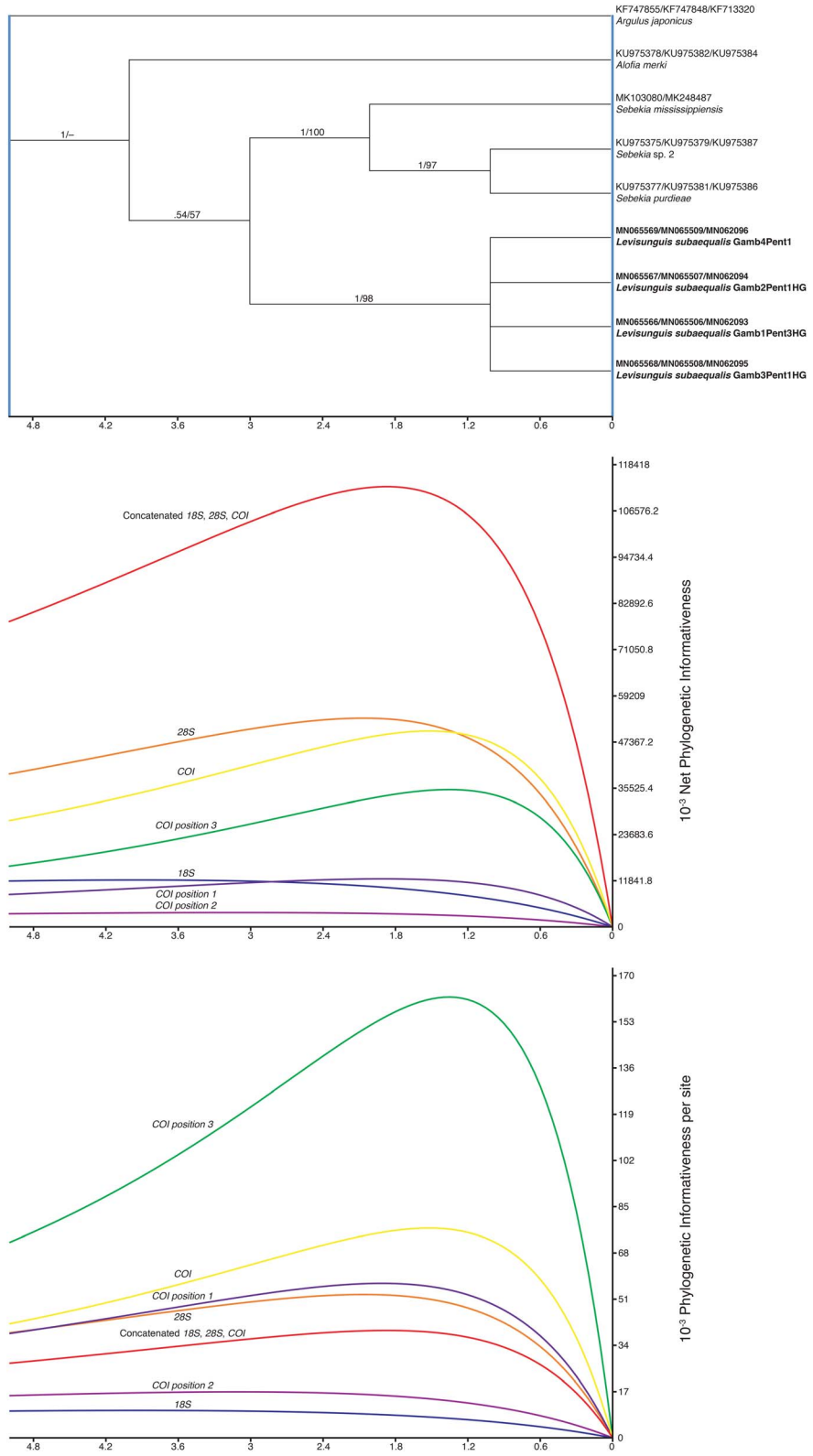

Figure 8. Net and per site phylogenetic informativeness profiles for *18S, 28S, COI,* each *COI* codon position, and concatenated sequence data from *18S, 28S,* and *COI* generated by PhyDesign. GenBank accession numbers are given for each sequence in the format *18S* accession number/*28S* accession number/*COI* accession number. Values above branches indicate posterior probabilities/bootstrap support values. Scale bar represents the number of nucleotide substitutions per site in the phylogenetic tree, while branch lengths are arbitrary in the morphology-based cladogram. Color version available online.

likelihood inference using all 3 regions are compelling enough to either support or refute the current, morphology-based classification of the Eupentastomida (Fig. 7). Single-locus analyses using all available sequence data for pentastomids from *18S, 28S,* and *COI* exhibit polytomies, polyphyletic clades, and low support values. Furthermore, these trees agree with neither each other nor the currently established, morphology-based placement of taxa within the class Eupentastomida. Only the concatenated analyses using *18S, 28S,* and *COI* data agree with currently accepted pentastomid taxonomy based on morphological characters. However, the bootstrap and posterior probability values are still low to offer robust support for the currently accepted taxonomy of this class. The wealth of phylogenetic trees recovered in the present study afforded some opportunity to offer a limited assessment of the phylogenetic signal from the *18S, 28S,* and *COI* regions as well as concatenated data from all 3 regions. Phylogenetic informativeness profiles constructed from each region using PhyDesign (Fig. 8) indicate the concatenated dataset offers the greatest net phylogenetic signal, with *28S* and *COI* providing the greatest single-locus contributions to net phylogenetic informativeness. *28S* offers greater informativeness at more basal clades, while *COI* offers slightly higher support at more distal branches. It is unfortunate that *28S,* the region that seems to offer the greatest phylogenetic signal of any single loci compared in the present study for distinguishing genera of pentastomids, is also the region with the least available data (Suppl. Table S1). Still, it must be noted that these analyses are based on the limited data presently available for these regions. More sequence data from *18S, 28S,* and *COI* are needed to more thoroughly assess the utility of these markers for phylogenetic inference of the evolutionary relationships between pentastomids. To date, only Barton and Morgan (2016) and Woodyard et al. (2019a) provide *18S, 28S,* and *COI* sequence data from the same specimens for 4 of the 141 currently described pentastomid species for the analyses carried out in the present study. While phylogenetic analyses using concatenated ribosomal and mitochondrial sequence data are increasingly being used for phylogenetic inference in other parasitic groups as evidenced by recent works on species ranging from Clinostomidae (Caffara et al., 2016; Woodyard et al., 2017; Briosio-Aguilar et al., 2019) to Emeriidae (Ogedengbe et al., 2018; Woodyard et al., 2019b), the present molecular data from pentastomids are not suitable for such analyses. While there are over 141 described pentastomid species belonging to 26 genera (Christoffersen and de Assis, 2013), molecular data, including the data from the present study, are publicly available for only 14 species from 11 genera. To this end, the authors urge any researchers undertaking molecular characterization of pentastomids to make publicly available sequence data from the *18S, 28S,* and *COI* genes to accommodate future studies. Although phylogenetic signal assessment in the current study suggests these regions have the most phylogenetic utility when combined, the respective phylogenetic utilities of these regions, either alone or in combination, are not yet well established for pentastomids. While the present molecular analyses cannot be said to definitively support the placement of the genus *Levisunguis* within the family Sebekidae, as established based on the morphological assessment by Curran et al. (2014) and the present study, there is little reason to doubt the current placement of the genus. Nonetheless, it is clear that data from other pentastomid taxa are needed to further infer the phylogeny of these enigmatic parasites.

ACKNOWLEDGMENTS

This work was supported by the Colleges of Veterinary Medicine at Mississippi State University and the University of Georgia. This work was also supported by the 2018 Student Subunit of the American Fisheries Society at Mississippi State University by an Undergraduate Research Scholarship awarded to E.T.W. and the 2018 Mississippi Chapter of the American Fisheries Society Student Research Scholarship, also awarded to E.T.W.

LITERATURE CITED

Almeida, W. O., and M. L. Christoffersen. 1999. A cladistic approach to relationships in Pentasomida. Journal of Parasitology 85: 695–704.

Altekar, G., S. Dwarkadas, J. P. Huelsenbeck, and F. Ronquist. 2004. Parallel metropolis coupled Markov chain Monte Carlo for Bayesian phylogenetic inference. Bioinformatics 20: 407–415.

Barton, D. P., and J. A. T. Morgan. 2016. A morphological and genetic description of pentastomid infective nymphs belonging to the family Sebekidae Sambon, 1922 in fish in Australian waters. Folia Parasitologica 63: 026. doi:10.14411/fp.2016.026.

Boschung, H. T., and R. L. Mayden. 2004. Fishes of Alabama. Smithsonian Books, Washington, DC, 736 p.

Boyko, C. B. 1996. Catalog of recent type specimens in the Department of Invertebrates, 671 American Museum of Natural History. III. "Parasitica" (phyla Platyhelminthes, Rhombozoa, and 672 Pentastomida) and Gastrotricha (supplement). American Museum Novitates 3174: 1–59.

Briosio-Aguilar, R., M. García-Varela, D. I. Hernández-Mena, M. Rubio-Godoy, and G. Pérez-Ponce de León. 2019. Morphological and molecular characterization of an enigmatic clinostomid trematode (Digenea: Clinostomidae) parasitic as metacercariae in the body cavity of freshwater fishes (Cichlidae) across Middle America. Journal of Helminthology 93: 461–474.

Bush, A. O., K. D. Lafferty, J. M. Lotz, and A. W. Shostak. 1997. Parasitology meets ecology on its own terms: Margolis et al. revisited. Journal of Parasitology 83: 575–583.

Caffara, M., S. A. Locke, C. Cristanini, N. Davidovich, M. P. Markovich, and M. L. Fioravanti. 2016. A combined morphometric and molecular approach to identifying metacercariae of *Euclinostomum heterostomum* (Digenea: Clinostomidae). Journal of Parasitology 102: 239–248.

Carpenter, N. 2018. Variation in helminth parasite component communities of *Gambusia affinis* and the effect of parasitism on host fitness. M.S. Thesis. Tarleton State University, Stephenville, Texas, 41 p.

Christoffersen, M. L., and J. E. de Assis. 2013. A systematic monograph of the recent Pentastomida with a compilation of their hosts. Zoologische Mededelingen 87: 1–206.

Christoffersen, M. L., and J. E. de Assis. 2015. Class Eupentastomida Waloszek, Repetski & Maas, 2006. *In* Treatise on zoology—Anatomy, taxonomy, biology. The Crustacea, Vol. 5, J. C. von Vapuel Klein, M. Charmantier-

Daures, and F. R. Schram (eds.). Brill Publishers, Leiden, the Netherlands, p. 5–75.

Clopper, C., and E. S. Pearson. 1934. The use of confidence or fiducial limits illustrated in the case of the binomial. Biometrika 26: 404–413.

Curran, S. S., R. M. Overstreet, D. E. Collins, and G. W. Benz. 2014. *Levisunguis subaequalis* n. g., n. sp., a tongue worm (Pentastomida: Porocephalida: Sebekidae) infecting softshell turtles, *Apalone* spp. (Testudines: Trionychidae) in the southeastern United States. Systematic Parasitology 87: 33–45.

Dreyer, H., and J.-W. Wägele. 2001. Parasites of crustaceans (Isopoda: Bopyridae) evolved from fish parasites: molecular and morphological evidence. Zoology 103: 157–178.

Fain, A. 1961. Les pentastomides de l'Afrique central. Annales Musée Royal de l'Afrique Central Série 8 no. 92: 1–115.

Folmer, O., M. Black, W. Hoeh, R. Lutz, and R. Vrijenhoek. 1994. DNA primers for amplification of mitochondrial cytochrome c oxidase subunit I from diverse metazoan invertebrates. Molecular Marine Biology and Biotechnology 3: 294–299.

Hwang, U. W., and W. Kim. 1999. General properties and phylogenetic utilities of nuclear ribosomal DNA and mitochondrial DNA commonly used in molecular systematics. Korean Journal of Parasitology 37: 215–228.

Junker, K. 2002. A study on the Pentastomida parasitizing crocodilian and chelonian final hosts, with special emphasis on the South African pentastome fauna. Ph.D. Dissertation. University of Karlsruhe, Gütersloh, North Rhine-Westphalia, Germany, 212 p.

Katoh, K., and D. M. Standley. 2013. MAFFT multiple sequence alignment software version 7: Improvements in performance and usability. Molecular Biology and Evolution 30: 772–780.

Kearse, M., R. Moir, A. Wilson, S. Stones-Havas, M. Cheung, S. Sturrock, S. Buxton, A. Cooper, S. Markowitz, C. Duran, et al. 2012. Geneious Basic: An integrated and extendable desktop software platform for the organization and analysis of sequence data. Bioinformatics 28: 1647–1649.

Kim, M. K., K. H. Pyo, Y. S. Hwang, H. S. Chun, K. H. Park, S. H. Ko, J. Y. Chai, and E. H. Shin. 2013. Effect of citric acid on the acidification of artificial pepsin solution for metacercariae isolation from fish. Veterinary Parasitology 198: 111–115.

Kumar, S., G. Stecher, and K. Tamura. 2016. MEGA7: Molecular evolutionary genetics analysis version 7.0 for bigger datasets. Molecular Biology and Evolution 33: 1870–1874.

Landan, G., and D. Graur. 2008. Local reliability measures from sets of co-optimal multiple sequence alignments. Pacific Symposium on Biocomputing 13: 15–24.

Littlewood, D. T. J., M. Curini-Galletti, and E. A. Herniou. 2000. The interrelationships of Proseriata (Platyhelminthes: Seriata) tested with molecules and morphology. Molecular Phylogenetics and Evolution 18: 449–466.

López-Giráldez, F., and J. P. Townsend. 2011. PhyDesign: An online application for profiling phylogenetic informativeness. BMC Evolutionary Biology 11: 152. doi:10.1186/1471-2148-11-152.

Maddison, W. P., and D. R. Maddison. 2018. Mesquite: a modular system for evolutionary analysis. Available at: http://www.mesquiteproject.org. Accessed 14 June 2019.

Nguyen, L. T., H. A. Schmidt, A. von Haeseler, and B. Q. Minh. 2015. IQ-TREE: A fast and effective stochastic algorithm for estimating maximum-likelihood phylogenies. Molecular Biology and Evolution 32: 268–274.

Ogedengbe, M. E., S. El-Sherry, J. D. Ogedengbe, H. D. Chapman, and J. R. Barta. 2018. Phylogenies based on combined mitochondrial and nuclear sequences conflict with morphologically defined genera in the eimeriid coccidia (Apicomplexa). International Journal for Parasitology 48: 56–69.

Overstreet, R. M., J. T. Self, and K. A. Vliet. 1985.The pentastomid *Sebekia mississippiensis* sp. n. in the American alligator and other hosts. Proceedings of the Helminthological Society of Washington 52: 266–277.

Poore, G. C. B. 2012. The nomenclature of the recent Pentastomida (Crustacea) with a list of species and available names. Systematic Parasitology 82: 211–240.

Rambaut, A. 2016. FigTree. Available at: http://tree.bio.ed.ac.uk/software/figtree/. Accessed 21 July 2017.

Raupach, M. J., C. Mayer, M. Malyutina, and J.-W. Wägele. 2009. Multiple origins of deep-sea *Asellota* (Crustacea: Isopoda) from shallow waters revealed by molecular data. Proceedings of the Royal Society B: Biological Sciences 276: 799–808.

Ronquist, F., and J. P. Huelsenbeck. 2003. MRBAYES 3: Bayesian phylogenetic inference under mixed models. Bioinformatics 19: 1572–1574.

Rosser, T. G., N. R. Alberson, E. T. Woodyard, F. L. Cunningham, L. M. Pote, and M. J. Griffin. 2017. *Clinostomum album* n. sp. and *Clinostomum marginatum* (Rudolphi, 1819), parasites of the great egret *Ardea alba* L. from Mississippi, USA. Systematic Parasitology 94: 35–49.

Rózsa, L., J. Reiczigel, and G. Majoros. 2000. Quantifying parasites in samples of hosts. Journal of Parasitology 86: 228–232.

Sela, I., H. Ashkenazy, K. Katoh, and T. Pupko. 2015. GUIDANCE2: Accurate detection of unreliable alignment regions accounting for the uncertainty of multiple parameters. Nucleic Acids Research 43: W7–W14.

Sheehan, D. C., and B. B. Hrapchak. 1980. Connective tissue and muscle fiber stains. *In* Theory and practice of histotechnology, 2nd ed. C. V. Mosby, St. Louis, Missouri, p. 180–201.

Tkach, V. V., D. T. J. Littlewood, P. D. Olson, J. M. Kinsella, and S. Zdzislaw. 2003. Molecular phylogenetic analysis of the Microphalloidea Ward, 1901 (Trematoda: Digenea). Parasitology 56: 1–15.

Trifinopoulos, J., L. T. Nguyen, A. von Haeseler, and B. Q. Minh. 2016. W-IQ-TREE: A fast online phylogenetic tool for maximum likelihood analysis. Nucleic Acids Research 44: W232–W235.

Woodyard, E. T., W. A. Baumgartner, T. G. Rosser, E. N. Bodin, A. M. Ferrara, T. W. Noto, L. M. Ford, and S. A. Rush. 2019a. Morphological, molecular, and histopathological data for *Sebekia mississippiensis* (Pentastomida: Sebekidae) Overstreet, Self, and Vliet, 1985 in the American alligator *Alligator mississippiensis* Daudin and the spotted

gar *Lepisosteus oculatus* Winchell. Journal of Parasitology 105: 283–298.

WOODYARD, E. T., T. G. ROSSER, AND S. A. RUSH. 2017. Alligator wrestling: Morphological, molecular, and phylogenetic data on *Odhneriotrema incommodum* (Leidy, 1856) (Digenea: Clinostomidae) from *Alligator mississippiensis* Daudin, 1801 in Mississippi, USA. Parasitology Research 116: 2981–2993.

WOODYARD, E. T., S. A. RUSH, AND T. G. ROSSER. 2019b. Redescription of *Eimeria megabubonis* Upton, Campbell, Weigel, & McKown 1990 (Apicomplexa: Emeriidae) from the great horned owl *Bubo virginianus* (Gmelin). Systematic Parasitology 96: 585–594.

XIA, X. 2018. DAMBE7: New and improved tools for data analysis in molecular biology and evolution. Molecular Biology and Evolution 35: 1550–1552.